CHAPTER 1

GENERAL INTRODUCTION

1.1 USING THE MOUSE AS A GENETIC TOOL

Mice have frequently been used to model both normal human development and human diseases. This is because they share many similarities with humans, both in terms of physiology and anatomy. Other features that make mice a great model organism include a small body size (which allows them to be housed at high density and makes them easy to handle), a short gestation time and prolificacy in breeding (allowing the generation of a study cohort within a short period of time). The finding that more than 90% of the human and mouse genomes can be divided into regions of conserved synteny, and that about 99% of mouse genes have homologues in the human genome (Waterston 2002) is further evidence that the mouse represents a good model to study human development.

The isolation of pluripotent mouse embryonic stem (ES) cells (Evans 1981), successful regeneration of germ line and somatic tissues from cultured ES cells reintroduced into the blastocyst (Bradley 1984) and the development of chromosome engineering techniques allowing the generation of defined chromosomal rearrangements (Ramirez-Solis 1995) mark key developments in the ability to use the mouse as a genetic tool.

1.2 CHROMOSOME ENGINEERING IN MOUSE ES CELLS

1.2.1 WAYS OF INDUCING CHROMOSOMAL REARRANGENTS IN MICE

Chromosomal rearrangements in mice can be randomly generated by ionizing radiation or exposure to chemical mutagens, such as ethylene oxide

or chlorambucil (Stubbs 1997) (however, the endpoints of such rearrangements cannot be predetermined) or can be precisely introduced into a defined genomic location using chromosome engineering techniques (Ramirez-Solis 1995).

1.2.2 A BRIEF OVERVIEW OF CHROMOSOME ENGINEERING IN MOUSE ES CELLS

Chromosome engineering utilizes the combination of ES cell gene targeting and the Cre/*loxP* site-specific recombination system to generate a defined chromosomal rearrangement (Ramirez-Solis 1995). Briefly, two *loxP* (locus of crossover P1) recombinase recognition sites are sequentially targeted in two predefined loci in the mouse ES cell genome. Subsequently, the expression of Cre, a recombinase that binds to a 13 basepair (bp) sequence flanking the 8 bp core spacer sequence of *loxP* (Sauer 1988), induces targeted recombination between the two *loxP* sites to generate the chromosomal rearrangement.

1.2.3 A STRATEGY TO GENERATE CHROMOSOMAL REARRANGENTS IN MOUSE ES CELLS

The selection of two endpoints is the first step to generating a chromosomal rearrangement. Both genes of known chromosomal location and simple sequence length polymorphism (SSLP) microsatellite markers have been successfully used as endpoints for generating chromosomal rearrangements (Lindsay 1999; Zheng 2000). The next step involves the insertion of a targeting vector containing a *loxP* site, a positive selection cassette (e.g. neomycin), a coat-colour marker (e.g. tyrosinase minigene) and one of two complementary, but independently non-functional, parts of a hypoxanthine phosphoribosyl transferase (*Hprt*) mini-gene (either 5'*Hprt* or 3'*Hprt*) into the first chosen endpoint (Ramirez-Solis 1995; Zheng 1999) (**Figure 1.1**). The successful insertion of the targeting vector into the first endpoint can be identified by positive selection (only the ES cell clones that express the positive selectable marker gene, e.g. the neomycin resistance gene, will survive the selection in a culture medium supplemented with this drug), and subsequently confirmed by either Southern blot analysis or

polymerase chain reaction (PCR). The single-targeted ES cell clones are subsequently targeted with a second vector containing a *loxP* site, a different positive selection cassette (e.g. puromycin), a different coat-colour marker (e.g. K14-agouti transgene) and the complimentary part of the *Hprt* gene into the second chosen endpoint (**Figure 1.1**). As in the case of the first targeting vector, the successful insertion of the targeting vector into the second endpoint can be identified by positive selection, and subsequently confirmed by either Southern blot analysis or PCR. Finally, the double-targeted ES cell clones are electroporated with a Cre-expression vector, e.g. pOG231 (O'Gorman 1997), in order to induce a recombination between two *loxP* sites. Following the electroporation, the ES cell clones are cultured in a medium supplemented with hypoxanthine, aminopterin and thymidine (HAT) in order to select the positive recombinant ES cell clones in which, as a consequence of Cre-mediated recombination, the two parts of the *Hprt* mini-gene have been brought together, making a functional gene. The successful generation of the chromosomal rearrangement can be confirmed by fluorescence in situ hybridization analysis (FISH). Finally, the ES cell clones carrying the engineered rearrangement are injected into mouse blastocysts to generate chimaeras, from which the progeny carrying the chromosomal rearrangement are derived.

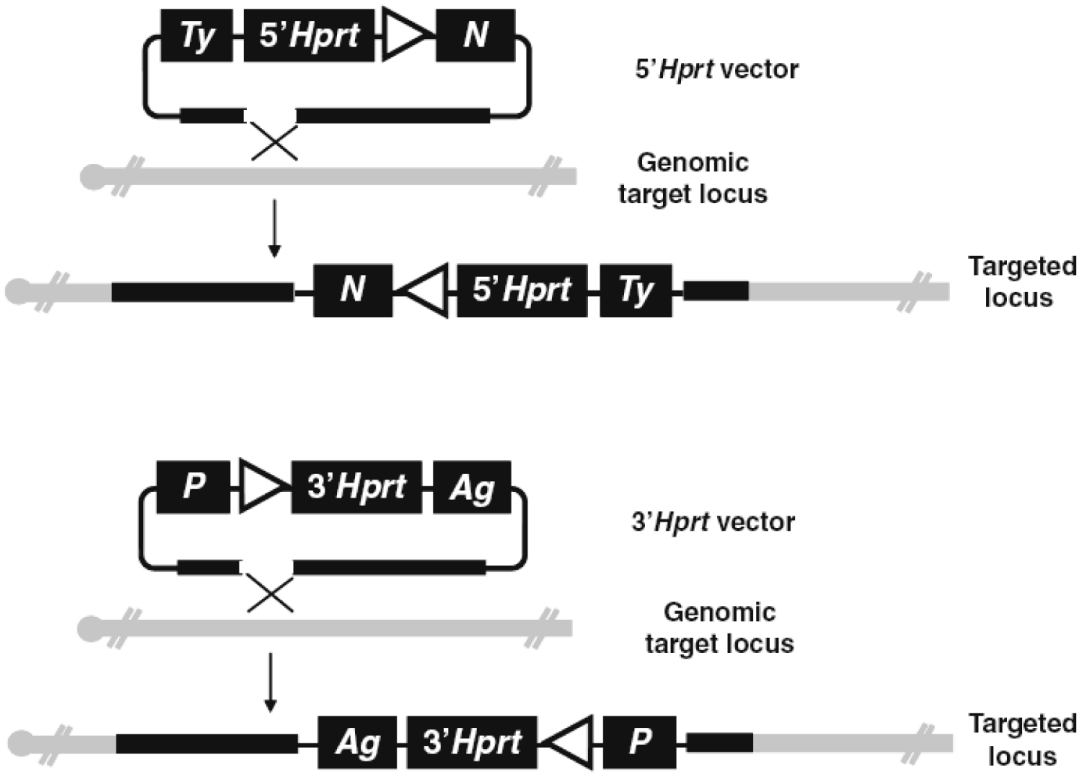

Figure 1.1. Gene targeting in ES cells. Insertional targeting vectors can be used to insert *loxP* sites, positive selectable markers, hypoxanthine phosphoribosyltransferase (*Hprt*) gene fragments and coat-colour markers to predetermined loci in the ES cell genome. The vector (thin black line) is linearized in the region of homology (thick black line) to stimulate targeted insertion into the locus (thick grey line). The 5'*Hprt* vector contains the neomycin selectablemarker (*N*), the 5' end of the *Hprt* minigene, a *loxP* site (white triangle) and the tyrosinase minigene (*Ty*) coat-colour marker. The 3'*Hprt* vector contains the puromycin selectable marker (*P*), the 3' end of the Hprt minigene, a *loxP* site (white triangle) and the agouti (*Ag*) coat-colour marker. Figure taken from van der Weyden *et al*., 2009.

1.2.4 TYPES OF CHROMOSOMAL REARRANGEMENTS GENERATED IN MOUSE ES CELLS

The type of chromosomal rearrangement that is generated in double-targeted ES cells depends on the *loxP* sites orientation, the localization of both *loxP* sites on the same or different chromosomes, and the relative configuration of the two parts of the *Hprt* gene (Ramirez-Solis 1995) (**Figure 1.2, 1.3, 1.4**). *LoxP* sites inserted in the same orientation on the same chromosome result in the generation of a chromosomal deletion, while *loxP* sites inserted in the same orientation on homologous chromosomes result in the generation of chromosomal deletion and duplication (**Figure 1.2**). *LoxP*

sites inserted in the opposite orientation on the same chromosome result in the generation of chromosomal inversion (**Figure 1.3**), whereas *loxP* sites inserted in the same orientation on non-homologous chromosomes result in the generation of chromosomal translocation (**Figure 1.4**).

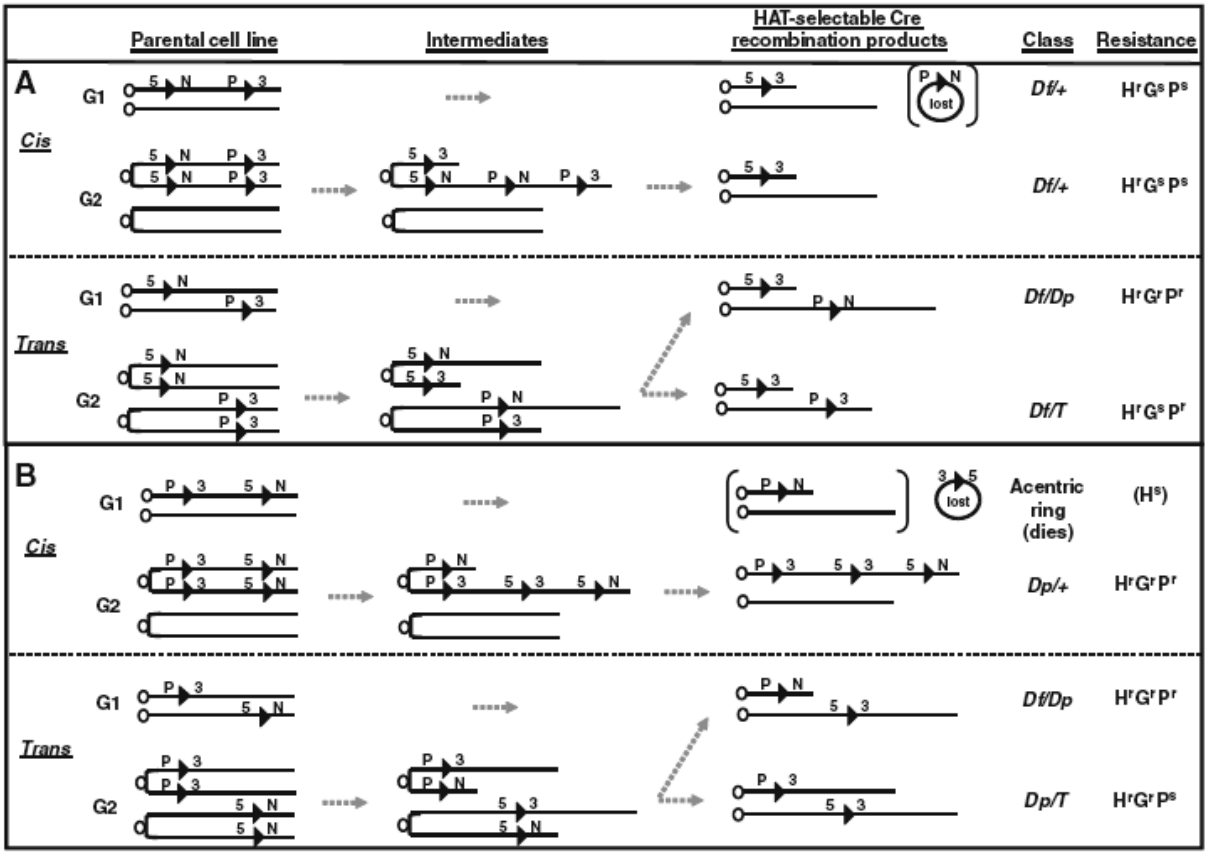

Figure 1.2. Engineering a deletion and/or duplication in embryonic stem cells. When the two *loxP* sites are targeted in the same orientation with respect to the centromere, the half *Hprt* cassettes can lie in two orientations, **(A)** outside the floxed region or **(B)** inside the floxed region. G1 and G2 indicate the different phases of the cell cycle in which recombination occurs. For G2 events, only recombination between *loxP* sites on different chromatids is considered: G2 recombination can also occur between two *loxP* sites on the same chromatid, but these events have the same consequence as the corresponding G1 events and are therefore not shown. The resulting recombination products and hence drug sensitivity (''resistance'') will depend upon whether the *loxP* sites are located in cis (on the same chromosome) or trans (on the two chromosome homologs). Note that using the strategy described in the text, only viable HAT-resistant recombination products are recovered and scored (those products shown in brackets are not HAT selectable). A *loxP* site is indicated by a black triangle, a centromere is indicated by an open circle. Abbreviations: 5, 5'*Hprt* cassette; 3, 3'*Hprt* cassette; *Df*, deficiency (deletion); *Dp*, duplication; G, G418 (neomycin); H, HAT (hypoxanthine, aminopterin and thymidine); N, neomycin selection cassette (conferring resistance to G418); P, puromycin selection cassette (conferring resistance to puromycin); r, resistant; s, sensitive; *T*, targeted. Figure taken from van der Weyden *et al*., 2009.

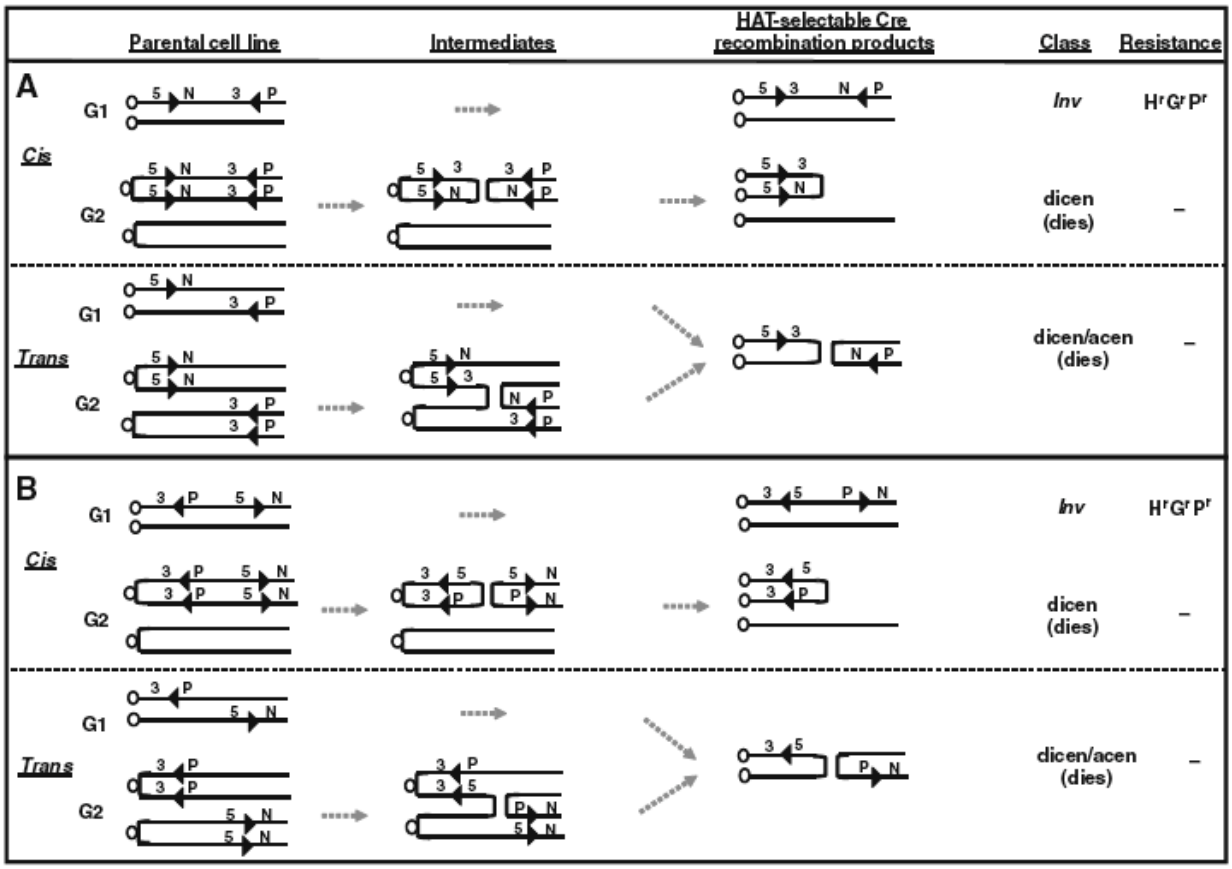

Figure 1.3. Engineering an inversion in embryonic stem cells. When the two *loxP* sites are targeted in the opposite orientation with respect to the centromere, either **(A)** facing towards or **(B)** away from each other, a chromosomal inversion will only occur if the loxP sites are in cis (on the same chromosome). Note that using the strategy described in the text, only viable HAT-resistant recombination products are recovered and scored. Details of the abbreviations and symbols are the same as for **Figure 1.2** (with additional abbreviations: acen, acentric; dicen, dicentric). Figure taken from van der Weyden *et al*., 2009.

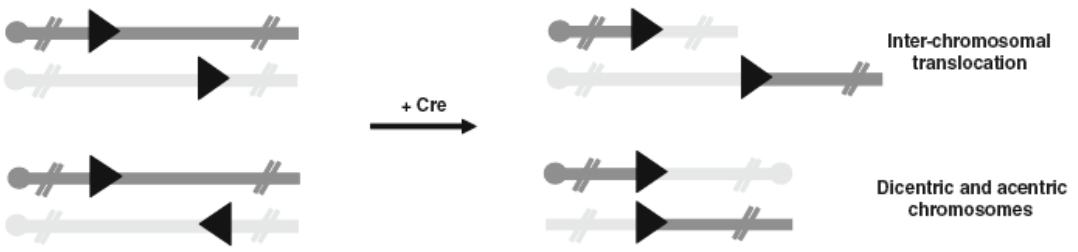

Figure 1.4. Engineering chromosomal translocations. Cre-mediated recombination leads to chromosomal translocation or dicentric and acentric chromosomes, depending on the relative orientations of the *loxP* sites (black triangles) on two non-homologous chromosomes. Figure taken from van der Weyden *et al*., 2009.

1.2.5 TARGETING VECTORS USED TO GENERATE CHROMOSOMAL REARRANGEMENTS IN MOUSE ES CELLS

Two complementary libraries *(*5'*Hprt* and 3'*Hprt*) consisting of insertion targeting vectors have been developed to facilitate the generation of chromosome rearrangements in the mouse ES cells (Zheng 1999). The insertion targeting vectors have been developed by cloning a 129S5/SvEvBrd genomic DNA genomic library into one of two vector backbones, containing either a *loxP* site, a 5' fragment of the *Hprt* gene, a positive selection cassette (neomycin; PGK-neo-bpA) and a coat-colour marker (tyrosinase minigene; *Ty*; resulting in greyish coat on an otherwise albino background) (Yokoyama 1990; Overbeek 1991) or a *loxP* site, a 3' fragment of the *Hprt* gene, a positive selection cassette (puromycin; PGK-puro-bpA) and a coat-colour marker (K14-agouti transgene; *Ag*; resulting in ''butterscotch'' coat in black agouti or non-agouti mice) (Kucera 1996). Each of these insertion targeting vectors requires only linearization within its genomic insert prior to electroporation into the ES cells (Zheng 1999). Moreover, the genomic insert in all of the available insertion targeting vectors is flanked by *Asc*I restriction enzyme sites, which allows inversion of the orientation of the genomic insert relative to the vector backbone or shuttling of the genomic insert between different vector backbones if needed (Zheng 1999).

A great advance in using these two libraries has been achieved by end-sequencing and mapping more than 150,000 clones (insertion targeting vectors) against the genome. All the data is available via the Mutagenic Insertion and Chromosome Engineering Resource (MICER) (htpp://www.sanger.ac.uk/PostGenomics/mousegenomics) (Adams 2004). Moreover, all mapped clones can be found in the Ensembl genome browser (Hubbard 2007) under the DAS source "MICER".

1.3 CHROMOSOMAL REARRANGEMENTS IN HUMANS

1.3.1 TYPES OF CHROMOSOMAL REEARANGEMENTS FOUND IN HUMANS

Unbalanced structural chromosomal abnormalities, ranging from the gain or loss of an entire chromosome to the gain or loss of a small chromosome fragment, are detected in about 3% of all human individuals, while balanced structural chromosomal anomalies, including inversions, translocations and ring chromosomes, are detected in about 0.2% of all human individuals (Shaffer 2009). Altogether, this makes germline and somatic chromosomal abnormalities the most frequent cause of human genetic diseases. The most frequent type of somatic chromosomal abnormalities involves chromosomal translocations, a type of chromosomal rearrangement that is frequently found in human cancers, especially in leukaemias, lymphomas and sarcomas (Rabbitt 1994). On the other hand, the most common type of germline chromosomal abnormalities involves the gain or loss of sex chromosomes, with Triple-X syndrome being an example of the gain of one or more extra copies of the X chromosome in females (Tartaglia 2010) and Klinefelter syndrome being an example of the gain of one or more extra copies of the X chromosome in males (Wikström 2011), whilst Turner syndrome is an example of the loss of one copy of the X chromosome in females (Kesler 2007). The second most frequent type of germline chromosomal abnormalities involves triplication of autosomal chromosomes, with trisomy of chromosome 21 (Down syndrome) (Mégarbané 2009), 18 (Edwards syndrome) (Tucker 2007) and 13 (Patau syndrome) (Iliopoulos 2006) being the most common. However, less frequently occurring autosomal chromosomal deletions seem to have the most severe impact on phenotype, as they reveal both dosage-sensitive genes and recessive mutations, with a deletion of 1.5 – 3 Mb of the 22q11 region causing DiGeorge syndrome (Linday 2001), a deletion of around 5 – 7 Mb of the 15q11–q13 region causing Prader-Willi syndrome and Angleman syndrome (Buiting 2010), or a deletion of 3.7 Mb of the 17p11.2 region causing Smith-Magenis syndrome (Elsea 2008) being just a few examples.

1.3.2 MECHANISMS GENERATING CHROMOSOMAL REARRANGEMETS IN HUMANS

Two distinct mechanisms, namely non-allelic homologous recombination (NAHR) and non-homologous end joining (NHEJ), seem to be relevant for the occurrence of chromosomal rearrangements in humans.

Non-allelic homologous recombination is a form of homologous recombination that is responsible for the generation of the majority of recurrent rearrangements in the human genome (Gu, 2008). Such rearrangemets span the same genomic interval and are found in multiple individuals. NAHR occurs between low copy repeats (LCRs), which are blocks of DNA that show more than 95% sequence identity over at least 1 kb, but are not alleles (Gu, 2008). The alignment of two non-allelic LCRs during mitosis or meiosis followed by the subsequent crossover between them can lead to the generation of genomic rearangements in daughter cells (Gu, 2008). The resulting type of chromosomal rearrangement depends on the localization of both LCRs (whether they are on the same or different chromosomes) and their relative configuration. NAHR between two LCRs located on the same chromosome and in the same orientation leads to the generation of a chromosomal duplication and/or deletion, while NAHR between two LCRs located on the same chromosome but in the opposite orientation leads to invertion of the DNA fragment enclosed between the two LCRs. NAHR between two LCRs located on homologous chromosomes can result in the generation of chromosomal translocation (Gu, 2008). Moreover, exchanges of strands during NAHR tend to cluster in domains termed hotspots that are located within the LCRs. These hotspots are thought to be capable of inducing double-strand breaks (DSBs) (Gu, 2008).

Non-homologous end joining is one of the mechanisms involved in the repair of double-strand breaks in DNA and is also thought to be used in rejoining translocated chromosomes in cancer (Gu, 2008). NHEJ occurs between two DNA sequences that usually show only a very short homology (microhomology) (Gu, 2008). Such microhomologies are frequently present as single-stranded overhangs on both ends of the DSB. NHEJ consists of the detection of DSBs, bringing both ends of the break in close proximity, and modification of the broken DNA overhangs in such a way that they can be

subsequently ligated (Gu, 2008). Interestingly, many of the DSBs that are repaired by NHEJ occur within repetitive elements, including LTRs, long interspersed elements (LINEs) and *Alu* sequences, and in close proximity of particular DNA sequences, such as TTTAAA, that are thought to be capable of causing DSBs (Gu, 2008).

1.4 MODELLING HUMAN CHROMOSOMAL DELETIONS IN MICE

In order to make genotype-phenotype correlations and to get a better insight into the development and pathophysiology of human diseases that are caused by chromosomal deletions, as well as to facilitate the discovery of causative genes that are involved in these pathologies, different mouse models carrying defined chromosomal deletions have been successfully developed (Cattanach 1992; Jiang 1998; Yang 1998; Kimber 1999; Lindsay 1999; Tsai 1999; Puech 2000; Lindsay 2001; Merscher 2001; Walz 2003; Walz 2003; Yan 2004; Bi 2005; Ding 2005; Skryabin 2007; Li 2009).

1.4.1 DiGEORGE SYNDROME MOUSE MODELS

1.4.1.1 DiGEORGE SYNDROME

DiGeorge syndrome (DGS) is named after Dr Angelo DiGeorge who in 1968, described a group of infants with thymic aplasia, congenital hypoparathyroidism, hypocalcaemia, and immune deficiency (DiGeorge 1968). In addition, patients with DGS also show congenital cardiovascular anomalies, craniofacial abnormalities (receding or abnormally small jaw, widely spaced eyes, broad nasal root, midface hypoplasia, cleft palate (overt or submucosal), external ear anomalies), and behavioural defects. However, clinical symptoms in patients diagnosed with DGS show variable expressivity and severity (Linday 2001). DiGeorge syndrome is caused by a microdeletion of the 22q11 region, and together with velocardiofacial syndrome (VCFS) and conotruncal anomaly face syndrome, is classified as the ‘22q11 syndrome’

(Linday 2001). A deletion of a 3 Mb of the 22q11 region encompassing 30 genes is detected in approximately 90% of DGS patients, while a deletion of a 1.5 Mb of the 22q11 region encompassing 24 genes is detected in the remaining individuals (Linday 2001).

1.4.1.2 DiGEORGE SYNDROME (DGS) MOUSE MODELS

So far a few mouse models carrying deletions spanning different fragments of the A3 region of mouse chromosome 16 syntenic to the human 22q11 region have been developed (Kimber 1999; Lindsay 1999; Puech 2000; Lindsay 2001; Merscher 2001) (**Figure 1.5**). Each has been summarized in **Table 1.1** and will be discussed below in more detail.

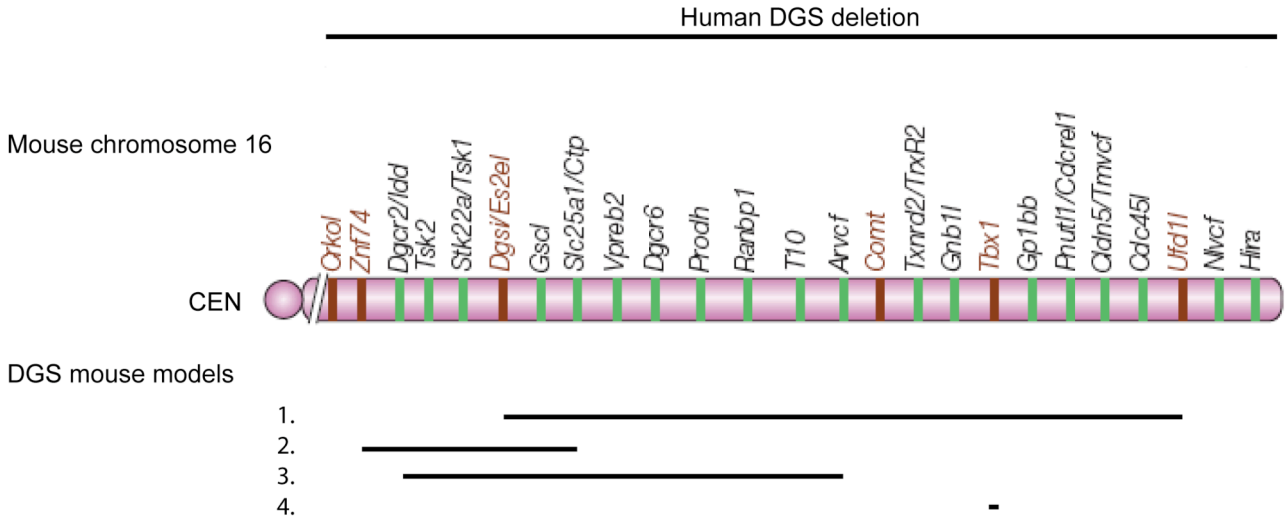

Figure 1.5. DGS mouse models that have been generated to date. Figure modified from Lindsay, 2001.
Legend: 1. Mouse model heterozygous for *Es2–Ufd1l* (*Df1* mouse model) (Lindsay 1999); 2. Mouse model heterozygous for *Znf74l–Ctp* (Kimber 1999); 3. Mouse model heterozygous for *Idd–Arvcf* (Puech 2000); 4. Mouse model heterozygous for*Tbx1* (Lindsay 2001; Merscher 2001).

Table 1.1. Brief summary of DGS mouse models that have been generated to date.

Clinical symptoms observed in humans with DGS	Mouse model heterozygous for *Es2–Ufd1l* (Lindsay 1999)	Mouse model heterozygous for *Znf74l–Ctp* (Kimber 1999)	Mouse model heterozygous for *Idd–Arvcf* (Puech 2000)	Mouse model heterozygous for*Tbx1* (Lindsay 2001; Merscher 2001)
Congenital cardiovascular abnormalities	+	-	-	+
Craniofacial abnormalities	-	-	-	Not reported
Thymic aplasia	-	-	-	Not reported
Behavioural problems	Not reported	+	Not reported	Not reported
Congenital hypoparathyroidism	-	-	-	Not reported
Hypocalcaemia	-	-	Not reported	Not reported
Immune deficiency	-	-	Not reported	Not reported

The first mouse model of DGS (*Df1*) carried a deletion of a 1.2 Mb of mouse chromosome 16, encompassing 22 genes, from *Es2* to *Ufd1l*, and was generated using chromosome engineering (Lindsay 1999) (**Figure 1.5**). Eighteen of these genes were homologous to genes deleted in patients carrying a 1.5 Mb deletion of the 22q11 region. Monosomic *Df1* mice (mice carrying a heterozygous deletion of the *Es2–Ufd1l* region) showed cardiovascular abnormalities, including an interrupted aortic arch type B, a ventricular septal defect and an aberrant right subclavian, similar to those diagnosed in human patients with DiGeorge syndrome. In order to test if haploinsufficiency of a gene (or genes) within the deleted region had a causative impact on the development of heart defects, a monosomic *Df1* deletion was genetically complemented with a reciprocal *Dp1* duplication in mice to restore a normal level of gene expression. The resulting mice were devoid of cardiovascular abnormalities, confirming that a gene (or genes) located within the *Df1* region is important in heart development.

The second mouse model of DGS carried a deletion of around 150 kb of mouse chromosome 16, encompassing 7 genes, from *Znf74l* to *Ctp*, and was generated using conventional replacement gene targeting techniques

(Kimber 1999) (**Figure 1.5**). Monosomic mice (mice carrying a heterozygous deletion of the *Znf74l–Ctp* region) did not display any cardiovascular abnormalities or other phenotypic anomalies observed in human patients with DiGeorge syndrome, but showed an increased prepulse inhibition of the startle response resembling reduced sensomotor gating observed in human patients with schizophrenia. Interestingly, 3 out of 7 genes deleted in these monosomic mice were shared with the monosomic *Df1* mice. This allowed exclusion of these 3 genes, namely *Idd*, *Tsk1* and *Tsk2*, as potential candidate genes for heart development as monosomic mice for the *Znf74l–Ctp* region did not show any cardiovascular defects observed in the monosomic *Df1* mice (Lindsay 1999).

The third mouse model of DGS carried a 550 kb deletion of mouse chromosome 16, encompassing 16 genes from *Idd* to *Arvcf*, and was generated using chromosome engineering (Puech 2000) (**Figure 1.5**). Monosomic mice (mice carrying a heterozygous deletion of the *Idd–Arvcf* region) did not show any cardiovascular defects or other phenotypic abnormalities diagnosed in human patients with DiGeorge syndrome. Interestingly, 13 out of 16 genes deleted in these monosomic mice were shared with the monosomic *Df1* mice. This allowed excluding these 13 genes (including e.g. *Idd*, *Tsk1* and *Tsk2* genes; see above (Kimber 1999)) as potential candidate genes for heart development, as monosomic mice for the *Idd–Arvcf* region did not display any cardiovascular defects, indicating that a candidate gene (or genes) responsible for the cardiovascular abnormalities must lie in the remaining 9 genes deleted in the monosomic *Df1* mice (Lindsay 1999).

Furthermore, the candidate gene approach led to the exclusion of two other genes, namely *Comt* and *Ufd1l*, as mice with mutations in these genes did not show any cardiovascular abnormalities (Puech 2000), while clinical data obtained from human patients identified with mutations in the *GP1Bb* gene allowed the exclusion of the *Gp1bb* gene as a candidate gene for heart development, as individuals with the mutation in the *GP1Bb* gene did not develop any cardiac defects (Puech 2000).

To identify which of the remaining 6 genes were responsible for the development of cardiovascular abnormalities present in human patients with DiGeorge syndrome, a series of genomic DNA fragments-rescue experiments was carried out (Lindsay 2001; Merscher 2001). This led to the identification of a critical region encompassing 4 genes (*Gnb1l, Tbx1, Gp1bb* and *Pnutl1*) that was sufficient to correct the cardiovascular abnormalities (Lindsay 2001; Merscher 2001). Finally, the T-box 1 (*Tbx1*) gene was selected for 'knocking out' because of its high expression in the pharyngeal arches and thus potentially important function in development of the heart (Lindsay 2001; Merscher 2001) (**Figure 1.5**). Indeed, mice carrying a heterozygous null mutation in the *Tbx1* gene displayed cardiovascular abnormalities identical to those observed in the monosomic *Df1* mice (Lindsay 1999), thus providing convincing evidence that haploinsufficiency of the *Tbx1* gene is responsible for cardiovascular defects observed in patients with DiGeorge syndrome (Lindsay 2001; Merscher 2001).

1.4.2 PRADER-WILLI SYNDROME AND ANGELMAN SYNDROME MOUSE MODELS

1.4.2.1 PRADER-WILLI SYNDROME AND ANGELMAN SYNDROME

Prader-Willi syndrome (PWS) is named after Professors Andrea Prader and Heinrich Willi who in 1956, described a group of children with short stature, growth retardation, obesity, small hands, and intellectual disability (Prader 1956). In addition, patients with PWS also show feeding difficulties and a failure to thrive during infancy, hypotonia, facial abnormalities (narrow bifrontal diameter, almond-shaped eyes, triangular mouth), hypogonadism and behavioural problems. The most common cause of PWS is a microdeletion within the paternal copy of the 15q11–q13 region (detected in about 70% of PWS cases), followed by a maternal uniparental disomy, imprinting defects (the paternal chromosome carries a maternal imprint) or chromosome translocations involving the paternal copy of the 15q11–q13 region (Buiting 2010). None of the genes mapped within the 15q11–q13

region have been found to be mutated in individuals with PWS, suggesting that PWS might be a continuous syndrome, in which loss of two or more paternally expressed genes act together to cause the PWS phenotype (Buiting 2010). Indeed, both microdeletions of the paternal 15q11–q13 region encompassing the *SNRPN* gene and microdeletions encompassing the paternally expressed *SNORD116* (*MBII-85*/*Pwcr1*) snoRNAs (small nucleolar RNAs, which are processed from the paternally expressed *SNURF–SNRPN* sense/*UBE3A* antisense transcript) have been detected in some individuals with PWS, suggesting that the deficiency of either the *SNRPN* gene or the *SNORD116* snoRNAs is responsible for the development of clinical features observed in patients with PWS (Buiting 2010). However, identification of balanced translocations that did not affect the expression of the *SNURF–SNRPN* gene, but separated the *SNORD116* snoRNAs from its promoter in patients with PWS allowed the exclusion of the *SNURF–SNRPN* as a candidate gene, providing further evidence that the deletion of the *SNORD116* snoRNAs was responsible for the development of the PWS phenotype in affected individuals (Buiting 2010).

Angelman syndrome (AS) is named after Dr Harry Angelman who in 1965, described a group of children with facial abnormalities, protruding tongues, and excessive laughter. Patients with AS also display microcephaly, profound intellectual disability, absence of speech, seizures, ataxic gait, and sleeping disorders. The most common cause of AS is a microdeletion within the maternal copy of the 15q11–q13 region (detected in about 70% of AS cases), followed by mutations in a maternal copy of the *UBE3A* gene, a paternal uniparental disomy, imprinting defects (the maternal chromosome carries a paternal imprint) or chromosome translocations involving the maternal copy of 15q11–q13 region (Buiting 2010). The loss of function of the maternally expressed *UBE3A* gene is now commonly accepted to be responsible for the development of clinical manifestations observed in patients with AS (Buiting 2010).

1.4.2.2 PRADER-WILLI SYNDROME (PWS) MOUSE MODELS

To date, a few mouse models for PWS have been developed. These models carried either a maternal duplication of the central fragment of the C region of mouse chromosome 7 syntenic to the human 15q11–q13 region or a paternal deletion spanning the C region of mouse chromosome 7 syntenic to the human 15q11–q13 region (Cattanach 1992; Yang 1998; Tsai 1999; Ding 2005; Skryabin 2007) (**Figure 1.6**). Each has been summarized in **Table 1.2** and will be discussed below in more detail.

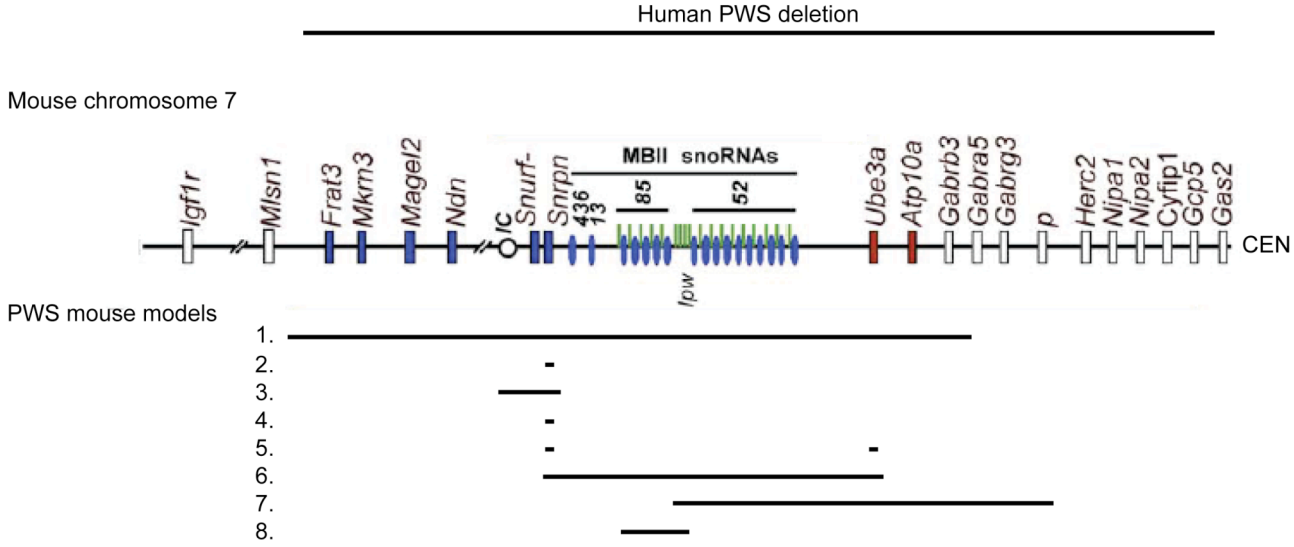

Figure 1.6. PWS mouse models that have been generated to date. Paternally, maternally, and biparentally expressed genes are labelled blue, red, and white, respectively. Figure modified from Skryabin *et al*., 2007.
Legend: 1. Mouse model carrying a maternal uniparental disomy of the central fragment of the C region of mouse chromosome 7 (Cattanach 1992); 2. Mouse model carrying a small intragenic deletion in the paternal copy of the *Snrpn* gene (Yang 1998); 3. Mouse model carrying a deletion of the paternal region of mouse chromosome 7 spanning the *Snrpn* gene and the distal portion of the putative mouse imprinting centre (IC) (Yang 1998); 4. Mouse model carrying a deletion of the exon 2 in the paternal copy of the *Snrpn* gene (Tsai 1999); 5. Mouse model targeted both for a deletion of the exon 2 in the paternal copy of the *Snrpn* gene and a deletion of the paternal copy of the *Ube3a* gene (Tsai 1999); 6. Mouse model carrying a deletion of the paternal region of mouse chromosome 7 from *Snrpn* to *Ube3a* inclusively (Tsai 1999); 7. Mouse model carrying a deletion of the paternal region of mouse chromosome 7 from the pink-eyed dilution (p) locus to undefined breakpoint between the *Snrpn* and *Ube3a* genes (Ding 2005); 8. Mouse model carrying a deletion spanning the paternal region of mouse chromosome 7 encompassing the *SNORD116* (*MBII-85*/*Pwcr1*) snoRNAs and exons A to C of the *Ipw* locus (Skryabin 2007).

Table 1.2. Brief summary of PWS mouse models that have been generated to date.

Clinical symptoms observed in humans with PWS	(1) First PWS mouse model (Cattanach 1992)	(2) Second PWS mouse model (Yang 1998)	(3) Third PWS mouse model (Yang 1998)	(4) Fourth PWS mouse model (Tsai 1999)
Intellectual disability	Not reported	Not reported	Not reported	Not reported
Behavioural problems	Not reported	Not reported	Not reported	Not reported
Feeding difficulties/ failure to thrive during infancy	+	-	+	-
Growth retardation/ short stature	+	-	+	-
Hypotonia	-	-	+	-
Hypogonadism	Not reported	-	-	-
Facial abnormalities	-	-	-	-
Obesity	Not reported	-	Not reported	-
Additional features not observed in humans with PWS			Unable to support themselves on their hind legs	

Legend: (1) First PWS mouse model carried a maternal uniparental disomy of the central fragment of the C region of mouse chromosome 7. (2) Second PWS mouse model carried a small intragenic deletion in the paternal copy of the *Snrpn* gene. (3) Third PWS mouse model carried a deletion of the paternal region of mouse chromosome 7 spanning the *Snrpn* gene and the distal portion of the putative mouse imprinting centre (IC). (4) Fourth PWS mouse model carried a deletion of the exon 2 in the paternal copy of the *Snrpn* gene.

Table 1.2 continued. Brief summary of PWS mouse models that have been generated to date.

Clinical symptoms observed in humans with PWS	(5) Fifth PWS mouse model (Tsai 1999)	(6) Sixth PWS mouse model (Tsai 1999)	(7) Seventh PWS mouse model (Ding 2005)	(8) Eight PWS mouse model (Skryabin 2007)
Intellectual disability	Not reported	Not reported	Not reported	Not reported
Behavioural problems	Not reported	Not reported	Not reported	Not reported
Feeding difficulties/ failure to thrive during infancy	-	+	-	+
Growth retardation/ short stature	-	+	-	+
Hypotonia	-	+	-	-
Hypogonadism	-	-	Not reported	-
Facial abnormalities	-	-	-	-
Obesity	-	-	-	-
Additional features not observed in humans with PWS		Decreased movements; impaired righting ability		

Legend: (5) Fifth PWS mouse model was targeted both for a deletion of the exon 2 in the paternal copy of the *Snrpn* gene and a deletion of the paternal copy of the *Ube3a* gene. (6) Sixth PWS mouse model carried a deletion of the paternal region of mouse chromosome 7 from *Snrpn* to *Ube3a* inclusively. (7) Seventh PWS mouse model carried a deletion of the paternal region of mouse chromosome 7 from the pink-eyed dilution (p) locus to undefined breakpoint between the *Snrpn* and *Ube3a* genes. (8) Eight PWS mouse model carried a deletion spanning the paternal region of mouse chromosome 7 encompassing the *SNORD116* (*MBII-85*/*Pwcr1*) snoRNAs and exons A to C of the *Ipw* locus.

The first mouse model of PWS carried a maternal uniparental disomy of the central fragment of the C region of mouse chromosome 7, and was generated by intercrossing heterozygous mice carrying reciprocal translocations (Cattanach 1992) (**Figure 1.6**). Mice with disomy died in early infancy, presumably due to suckling problems, which phenocopies the feeding difficulties observed in infants with PWS. However, considering that a large number of genes are located within the region of the maternal uniparental disomy, it was not possible to assign an observed phenotype to any particular gene.

The second mouse model of PWS carried a small intragenic deletion in the paternal copy of the *Snrpn* gene, and was generated using homologous

recombination (Yang 1998) (**Figure 1.6**). Mice with the heterozygous *Snrpn* deletion were viable and did not display any phenotypic abnormalities, suggesting that the deletion of the *Snrpn* gene is not sufficient to cause the PWS phenotype.

The third mouse model carried a deletion of the paternal region of mouse chromosome 7 spanning the *Snrpn* gene and the distal portion of the putative mouse imprinting centre (IC), and was generated using homologous recombination (Yang 1998) (**Figure 1.6**). The genomic sequence of the putative mouse IC was also encompassed into the engineered deletion because the human IC appears to control genomic imprinting of six paternally expressed transcripts that have been mapped to the human PWS/AS region (*SNRPN, ZNF217, NDN, IPW, PAR1, PAR5*), and deletions of the distal part of the IC have been reported in individuals with PWS (Yang 1998). Indeed, this deletion affected the imprinting of the region, as mice with this deletion lacked the transcription of the genes normally solely expressed from the paternal 15q11–q13 region, including *Zfp127*, *Ndn* and *Ipw*. At birth, monosomic mice (mice carrying a heterozygous deletion of the *Snrpn* gene and distal IC fragment) were underweight, slightly hypotonic and unable to support themselves on their hind legs, but otherwise normal. However, all of these monosomic mice died in early infancy (the majority died within first 72 hours) due to feeding difficulties and a failure to thrive that resembled observations from infants with PWS. As none of the monosomic mice survived till weaning, it was not possible to assess whether these mice would develop other symptoms observed in PWS patients, including hypogonadism or obesity later in their life.

The fourth mouse model of PWS carried a deletion of the exon 2 in either the paternal copy of the *Snrpn* gene, and was generated using chromosome engineering (Tsai 1999) (**Figure 1.6**). Importantly, this deletion did not affect the imprinting of the region. Mice with the deletion (heterozygous and homozygous) were viable and did not display any phenotypic abnormalities, suggesting that the deletion of the exon 2 of the *Snrpn* gene is not sufficient to cause the PWS phenotype.

The fifth mouse model of PWS was targeted both for a deletion of the exon 2 in the paternal copy of the *Snrpn* gene and a deletion of the paternal

copy of the *Ube3a* gene, and was generated using chromosome engineering (Tsai 1999) (**Figure 1.6**). Mice double-targeted for the *Snrpn* and *Ube3a* genes on the paternal chromosome were viable and did not display any phenotypic abnormalities, thus suggesting that a paternal deletion of the *Ube3a* gene is not important in the development of PWS manifestations.

The sixth mouse model of PWS carried a deletion of the paternal region of mouse chromosome 7 from *Snrpn* to *Ube3a* inclusively, and was generated using chromosome engineering (Tsai 1999) (**Figure 1.6**). Importantly, this deletion did not affect the imprinting of the genes located outside the deleted region. Monosomic pups (pups carrying a heterozygous deletion of the paternal *Snrpn–Ube3a* region) were underweight, showed hypotonia, decreased movements and inadequate feeding. The lethality during infancy and early adulthood was highly increased (80% of mice died before weaning), presumably due to failure to thrive. The monosomic mice that survived beyond weaning were fertile and did not develop obesity. Although the deficiency of a paternally expressed gene (or genes) in the *Snrpn–Ube3a* region is responsible for recapitulation of some PWS symptoms, the lack of other PWS manifestations, including hypogonadism and obesity, suggests the existence of significant developmental differences between mice and humans, as human PWS patients carrying a deletion within the *SNRPN–UBE3A* region displayed both hypogonadism and obesity (Buiting 2010).

The seventh mouse model of PWS (P^{30PUb}) carried a deletion of the paternal region of mouse chromosome 7 from the pink-eyed dilution (p) locus to an undefined breakpoint between the *Snrpn* and *Ube3a* genes, and was generated by ^{239}Pu citrate radiation (Ding 2005) (**Figure 1.6**). Monosomic P^{30PUb} mice were viable and did not display any phenotypic abnormalities. Further defining of the distal P^{30PUb} deletion breakpoints showed that the entire *SNORD115* (*MBII-52*) snoRNAs and *Ipw* locus, but not the *SNORD116* (*MBII-85*/*Pwcr1*) snoRNAs, were encompassed in the deletion region, suggesting that a gene (or genes) associated with the manifestation of the PWS phenotype is mapped between the *Snrpn* and *SNORD115* (*MBII-52*) snoRNAs, thus providing further evidence (in addition to currently available data for human patients with PWS; see above (Buiting 2010)) that the

deficiency of the *SNORD116* snoRNAs is responsible for the development of PWS symptoms.

The eighth mouse model of PWS (*PWScr*) carried a deletion spanning the paternal region of mouse chromosome 7 encompassing the *SNORD116* (*MBII-85*/*Pwcr1*) snoRNAs and exons A to C of the *Ipw* locus, and was generated using chromosome engineering (Skryabin 2007) (**Figure 1.6**). Monosomic *PWScr* pups (pups carrying a heterozygous deletion of the *SNORD116* and proximal part of the *Ipw* locus) were smaller than controls. They displayed postnatal growth retardation from a week of age due to poor feeding, but in contrary to the monosomic mice for the paternal *Snrpn–Ube3a* region (Tsai 1999), they showed only 15% postnatal lethality, thus suggesting that although the deficiency of *SNORD116* (*MBII-85*/*Pwcr1*) snoRNAs seems to be responsible for feeding difficulties, a gene (or genes) located between the *Snrpn* and *SNORD116* (*MBII-85*/*Pwcr1*) snoRNAs is causative for highly increased neonatal lethality in the monosomic mice for the paternal *Snrpn–Ube3a* region. Monosomic *PWScr* mice were fertile and did not develop obesity up to a year of age, but continued to be underweight compared to controls. This was in agreement with phenotypic observation in the monosomic mice for the paternal *Snrpn–Ube3a* region, which were also fertile and non-obese (Tsai 1999), and provided further evidence of the existence of significant developmental differences between mice and humans, as human PWS patients carrying a deletion within the *SNRPN–UBE3A* region, including deletions of only *SNORD116* (*MBII-85*/*PWCR1*) snoRNAs, displayed both hypogonadism and obesity (Buiting 2010).

1.4.2.3 ANGELMAN SYNDROME (AS) MOUSE MODELS

To date, a few mouse models for AS have been developed. These models carried either a paternal duplication of the central fragment of the C region of mouse chromosome 7 syntenic to the human 15q11–q13 region or a maternal deletion spanning the C region of mouse chromosome 7 syntenic to the human 15q11–q13 region (Cattanach 1992; Jiang 1998; Tsai 1999; Ding 2005) (**Figure 1.7**). Each has been summarized in **Table 1.3** and will be discussed below in more detail.

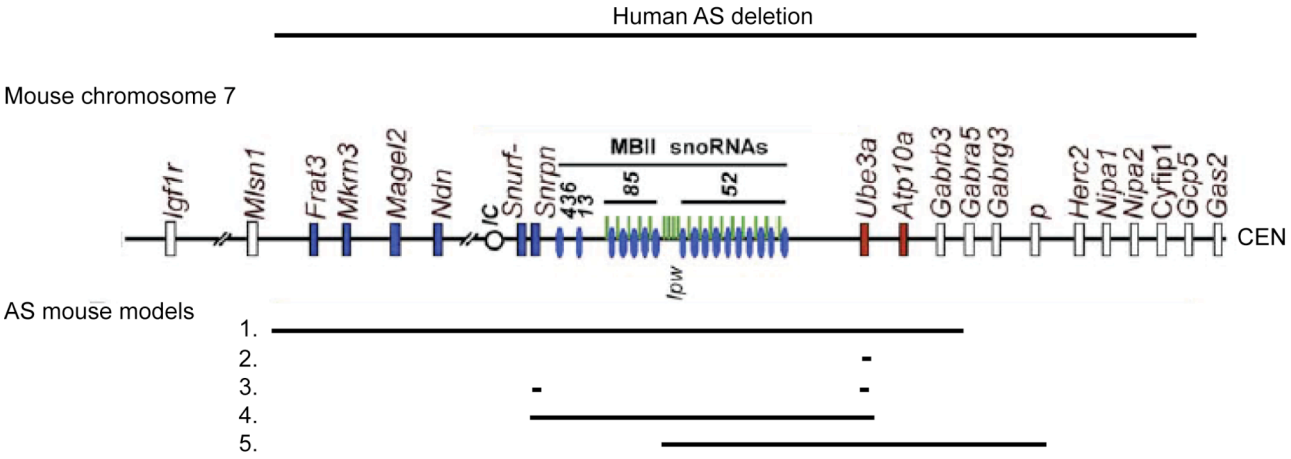

Figure 1.7. AS mouse models that have been generated to date. Paternally, maternally, and biparentally expressed genes are labelled blue, red, and white, respectively. Figure modified from Skryabin *et al*., 2007.
Legend: 1. Mouse model carrying one paternal and two maternal copies of the central fragment of the C region of mouse chromosome 7 (Cattanach 1992); 2. Mouse model carrying a null mutation in the maternal copy of the *Ube3a* gene (Jiang 1998); 3. Mouse model targeted both for a deletion of the exon 2 in the maternal copy of the *Snrpn* gene and a deletion of the maternal copy of the *Ube3a* gene (Tsai 1999); 4. Mouse model carrying a deletion of the maternal region of mouse chromosome 7 from *Snrpn* to *Ube3a*, inclusively (Tsai 1999); 5. Mouse model carrying a deletion of the maternal region of mouse chromosome 7 from the pink-eyed dilution (p) locus to undefined breakpoint between *Snrpn* and *Ube3a* genes (Ding 2005).

Table 1.3. Brief summary of AS mouse models that have been generated to date.

Clinical symptoms observed in humans with AS	(1) First AS mouse model (Cattanach 1992)	(2) Second AS mouse model (Jiang 1998)	(3) Third AS mouse model (Tsai 1999)	(4) Fourth AS mouse model (Tsai 1999)	(5) Fifth AS mouse model (Ding 2005)
Intellectual disability	Not reported	+	Not reported	Not reported	Not reported
Behavioural problems	Not reported	Not reported	Not reported	Not reported	Not reported
Facial abnormalities	Not reported	-	Not reported	Not reported	Not reported
Seizures	Not reported	+	Not reported	Not reported	Not reported
Sleeping disorder	Not reported	Not reported	Not reported	Not reported	Not reported
Ataxic gait	Not reported	-	Not reported	Not reported	Not reported
Microcephaly	Not reported	-	Not reported	Not reported	Not reported
Additional features not observed in humans with AS	Shorter tail length; growth retardation; failure to thrive	Motor impairment; reduction in skeletal size and overall body and brain weight			High-fat diet-induced obesity

Legend: (1) First AS mouse model carried one paternal and two maternal copies of the central fragment of the C region of mouse chromosome 7. (2) Second AS mouse model carried a null mutation in the maternal copy of the *Ube3a* gene. (3) Third AS mouse model was targeted both for a deletion of the exon 2 in the maternal copy of the *Snrpn* gene and a deletion of the maternal copy of the *Ube3a* gene. (4) Fourth AS mouse model carried a deletion of the maternal region of mouse chromosome 7 from *Snrpn* to *Ube3a*, inclusively. (5) Fifth AS mouse model carried a deletion of the maternal region of mouse chromosome 7 from the pink-eyed dilution (p) locus to undefined breakpoint between *Snrpn* and *Ube3a* genes.

The first mouse model of AS carried one paternal and two maternal copies of the central fragment of the C region of mouse chromosome 7, and was generated by intercrossing heterozygous mice carrying reciprocal translocations (Cattanach 1992) (**Figure 1.7**). These mice were smaller and showed reduced viability compared to controls. However, as the cause of their failure to thrive was not determined, it was not possible to speculate if these model recapitulated any aspects of AS.

The second mouse model of AS carried a null mutation in the maternal copy of the *Ube3a* gene, and was generated using chromosome engineering (Jiang 1998) (**Figure 1.7**). Mice with the *Ube3a* mutation displayed many symptoms observed in human patients with AS, including inducible seizures,

context-dependent learning dysfunction, behavioural defects, motor impairment, and reduction in skeletal size and brain weight.

The third mouse model of AS was targeted both for a deletion of the exon 2 in the maternal copy of the *Snrpn* gene and a deletion of the maternal copy of the *Ube3a* gene, and was generated using chromosome engineering (Tsai 1999) (**Figure 1.7**). Mice double-targeted for the *Snrpn* and *Ube3a* genes on the maternal chromosome were viable and were predicted to develop phenotypic abnormalities similar to those observed in mice carrying a null mutation in the *Ube3a* gene (Jiang 1998), though this was not assessed.

The fourth mouse model of AS carried a deletion of the maternal region of mouse chromosome 7 from *Snrpn* to *Ube3a* inclusively, and was generated using chromosome engineering (Tsai 1999) (**Figure 1.7**). Importantly, this deletion did not affect the imprinting of the genes located outside the deleted region. Monosomic mice (mice with carrying a heterozygous deletion of the maternal *Snrpn–Ube3a* region) were viable and did not show increased lethality. They were predicted to develop phenotypic abnormalities potentially resembling those observed in mice carrying a null mutation in the *Ube3a* gene (Jiang 1998), though this was not assessed.

The fifth mouse model of AS (P^{30PUb}) carried a deletion of the maternal region of mouse chromosome 7 from the pink-eyed dilution (p) locus to an undefined breakpoint between *Snrpn* and *Ube3a* genes, and was generated by ^{239}Pu citrate radiation (Ding 2005) (**Figure 1.7**). Monosomic P^{30PUb} mice were viable but developed obesity when fed on a high-fat diet due to the deletion of the *Atp10c* gene (a high-fat diet-induced obesity has been previously associated with the lack of the *Atp10c* expression), and were predicted to develop phenotypic abnormalities similar to those observed in mice carrying a null mutation in the *Ube3a* gene (Jiang 1998), as further defining of the distal P^{30PUb} deletion breakpoints showed that the *Ube3a* gene was encompassed in the deletion region, though this was not assessed.

1.4.3 SMITH-MAGENIS SYNDROME MOUSE MODELS

1.4.3.1 SMITH-MAGENIS SYNDROME

Smith-Magenis syndrome (SMS) is named after Drs Ann C. M. Smith and R. Ellen Magenis who in 1986, first described a group of children with brachycephaly, midface hypoplasia, prognathism, hoarse voice, speech delay with or without hearing loss, intellectual disability, growth impairment, and behavioural difficulties (Smith 1986). In addition to this, patients with SMS are also diagnosed with skeletal, eye, heart and kidney abnormalities, sleep disturbance, seizures, teenager and adult obesity, reduced pain and temperature perception, hypotonia, and chronic ear infections. The most common cause of SMS is an interstitial microdeletion of the 17p11.2 region, encompassing the retinoic acid-induced 1 (*RAI1*) gene (detected in about 90% of SMS cases), followed by mutations in the *RAI1* gene (detected in remaining 10% of SMS cases) (Elsea 2008). Approximately a 3.7 Mb deletion of the 17p11.2 region mediated through non-allelic homologous recombination between flanking low-copy repeats is detected in approximately 70% of SMS deletion patients. The remaining deletion SMS patients carry deletions spanning smaller or larger fragments of the 17p11.2 region derived from either alternative low-copy repeats or non-homologous recombination (Elsea 2008). Analysis of SMS patients carrying deletions spanning smaller fragments of the 17p11.2 region led to an identification of the SMS critical region (SMCR). Further analysis of the genes mapped within the SMCR in SMS individuals in whom the deletion of the 17p11.2 region was not detected resulted in identification of mutations within exon 3 of the *RAI1* gene, suggesting that haploinsufficiency of the *RAI1* gene is responsible for the development of the most typical clinical manifestations observed in SMS patients. However, other genes located within the SMCR are believed to modify the variability and degree of severity of SMS symptoms (Elsea 2008). Interestingly, patients carrying the reciprocal duplication of the 17p11.2 region have also been identified. However, the patients with 17p11.2 duplication display less severe symptoms than patients with SMS deletion, as there are observed only with

mild to borderline intellectual disability, and some behavioural abnormalities (Walz 2003).

1.4.3.2 SMITH-MAGENIS SYNDROME (SMS) MOUSE MODELS

So far a few mouse models carrying deletions spanning different fragments of the region of mouse chromosome 11 syntenic to the human 17p11.2 region have been developed (Walz 2003; Walz 2003; Yan 2004; Bi 2005) (**Figure 1.8**). Each has been summarized in **Table 1.4** and will be discussed below in more detail.

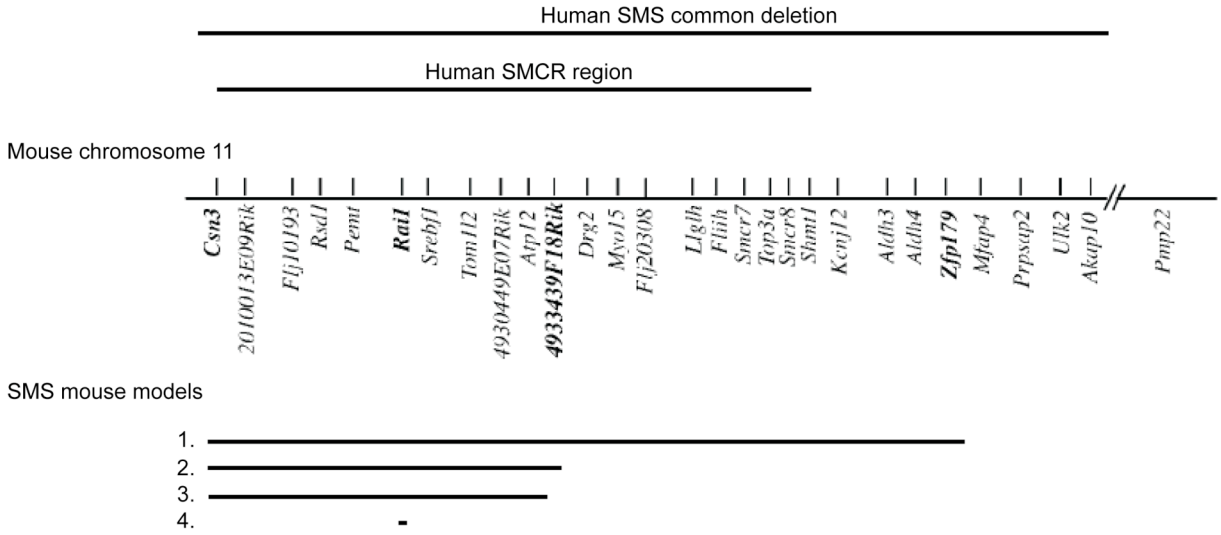

Figure 1.8. SMS mouse models that have been generated to date. Figure modified from Yan *et al*., 2004.
Legend: 1. *Df(11)17* mouse model (mouse model heterozygous for *Csn3–Zfp*) (Walz 2003; Walz 2003); 2. *Df(11)17-1* mouse model (Yan 2004); 3. *Df(11)17-2* mouse model (Yan 2004); 4. *Df(11)17-3* mouse model (Yan 2004); 5. Mouse model heterozygous for *Rai1* (Bi 2005).

Table 1.4. Brief summary of SMS mouse models that have been generated to date.

Clinical symptoms observed in humans with SMS	*Df(11)17* mouse model (Walz 2003; Walz 2003)	*Df(11)17-1* mouse model (Yan 2004)	*Df(11)17-2* mouse model (Yan 2004)	*Df(11)17-3* mouse model (Yan 2004)	Mouse model heterozygous for *Rai1* (Bi 2005)
Intellectual disability	-	Not reported	Not reported	Not reported	Not reported
Behavioural problems	+	Not reported	Not reported	Not reported	Not reported
Craniofacial abnormalities	+	+	+	+	+
Multiple organ abnormalities	-	-	-	-	Not reported
Seizures	+	-	-	-	Not reported
Hypotonia	Not reported	Not reported	Not reported	Not reported	Not reported
Sleeping disturbance	+	-	-	-	Not reported
Growth impairment	+	Not reported	Not reported	Not reported	+
Chronic ear infections	Not reported	Not reported	Not reported	Not reported	Not reported
Reduced pain and temperature perception	Not reported	Not reported	Not reported	Not reported	Not reported
Obesity	+	+	+	+	+
Additional features not observed in humans with SMS	Male-specific reduced fertility				

The first mouse model (*Df(11)17*) of SMS carried a 2 Mb deletion of mouse chromosome 11, from *Csn3* to *Zfp79* that was syntenic to the genomic interval most commonly deleted in SMS patients, and was generated using chromosome engineering (Walz 2003; Walz 2003) (**Figure 1.8**). Monosomic *Df(11)17* mice (mice carrying a heterozygous deletion of the *Csn3–Zfp79* region) recapitulated some of clinical features observed in SMS patients, including craniofacial abnormalities, growth impairment (up to 1 month of age), seizures, obesity (from 4 months of age), and abnormal circadian rhythm. Moreover, the monosomic *Df(11)17* males were also hypoactive and showed reduced fertility.

The subsequent three monosomic mouse models of SMS (*Df(11)17-1*, *Df(11)17-2* and *Df(11)17-3*) carried different sub-deletions of the genomic interval most commonly deleted in SMS patients (all of which included the *Rai1* gene), and were generated using retrovirual-mediated chromosome

engineering (Yan 2004) (**Figure 1.8**). All three monosomic mouse models displayed craniofacial abnormalities (however, the severity of craniofacial defects was much less pronounced than in the monosomic *Df(11)17* mice (Walz 2003)), and obesity, but did not show seizures or abnormal circadian rhythm. This confirms the existence of the SMCR which contains a gene (or genes), most likely the *Rai1* gene, that are sufficient to cause some of the SMS manifestations (Elsea 2008). However, other genes located within the genomic interval most commonly deleted in SMS patients are likely to both modify the degree of severity of craniofacial abnormalities and obesity and be responsible for the manifestation of other SMS symptoms.

In order to discriminate a role of the *Rai1* gene in the development of SMS phenotypes, including craniofacial abnormalities and obesity, a mouse model carrying a null mutation in the *Rai1* gene was generated using a candidate gene approach (Bi 2005) (**Figure 1.8**). Mice with the heterozygous *Rai1* mutation ($Rai^{+/-}$ mice) showed growth impairment between 4 to 7 weeks of age, were obese from 20 (males) or 23 (females) weeks of age, and showed craniofacial abnormalities similar to those observed both in humans and mice, confirming that a haploinsufficiency of the *Rai1* gene is sufficient to recapitulate some of the SMS phenotypes (Elsea 2008). However, the severity of craniofacial defects in the $Rai^{+/-}$ mice was similar to the monosomic *Df(11)17-1*, *Df(11)17-2* and *Df(11)17-3* mice (Yan 2004), but reduced in comparison to the monosomic *Df(11)17* mice (Walz 2003), further suggesting the influence of other genes located within the genomic interval most commonly deleted in SMS patients on the expressivity of craniofacial abnormalities and the variability of the other SMS manifestations.

In parallel with the generation of the monosomic *Df(11)17* mouse model, a mouse model (*Dp(11)17*) carrying a reciprocal 2 Mb duplication of mouse chromosome 11, from *Csn3* to *Zfp79*, that was syntenic to the genomic interval most commonly deleted in SMS patients was generated using chromosome engineering (Walz 2003). *Dp(11)17/+* mice (mice carrying a duplication of the *Csn3–Zfp79* region) were underweight, but did not display SMS features observed in the monosomic *Df(11)17* mice (Walz 2003), including craniofacial abnormalities, seizures or reduced male fertility. However, the *Dp(11)17/+* males were hyperactive, and showed learning

impairment in the contextual fear conditioning test (Walz 2003). Moreover, analysis of mice carrying both the deletion and reciprocal duplication (*Df(11)17/Dp(11)17*) revealed no apparent phenotypic abnormalities, suggesting that most of SMS abnormalities observed in the *Df(11)17/+* and *Dp(11)17/+* mice result from gene dosage imbalances (Walz 2003).

1.4.4 WILLIAMS SYNDROME MOUSE MODELS

1.4.4.1 WILLIAMS SYNDROME

Williams syndrome (known also as Williams-Beuren syndrome, WBS) is named after Dr J. C. P. Williams who in 1961, described a group of children with supravalvular aortic stenosis, craniofacial abnormalities (short cranial base, flat nasal bridge, periorbital fullness, malar flattening, short up-turned nose with anteverted nostrils, a long flat filtrum, full cheeks, prominent lips, wide mouth, small chin), and intellectual disability (Williams 1961). WBS patients also show weakness of connective tissues, short stature, reduced brain volume, motor impairment, and behavioural difficulties. The most common cause of the WBS is a 1.5 Mb microdeletion of the 7q11.23 region that is mediated through non-allelic homologous recombination between flanking low-copy repeats (Li 2009). This deletion encompasses 25 genes that are predominantly expressed in the brain. The phenotype-genotype correlation has so far been established for only one of these genes, namely the elastin (*ELN*) gene, whose deletion or disruption leads to supravalvular aortic stenosis, and thus is sufficient to cause a cardiac symptom observed in WBS patients (Li 2009).

1.4.4.2 WILLIAMS SYNDROME (WBS) MOUSE MODELS

So far several knock-out mouse models for different genes located within the genomic interval most commonly deleted in WBS patients have been developed (Li 2009). However, most of those mouse models, except for heterozygous *Cyln2* and heterozygous *Gtf2ird1* mouse models, either showed no phenotypical abnormalities or were not analysed (Hoogenraad 2002;

Young 2008; Li 2009) (**Figure 1.9**). Moreover, a few mouse models carrying deletions spanning different fragments of the G2 region of mouse chromosome 5 syntenic to the human 7q11.23 region have been developed (Li 2009) (**Figure 1.9**). Each has been summarized in **Table 1.5** and will be discussed below in more detail.

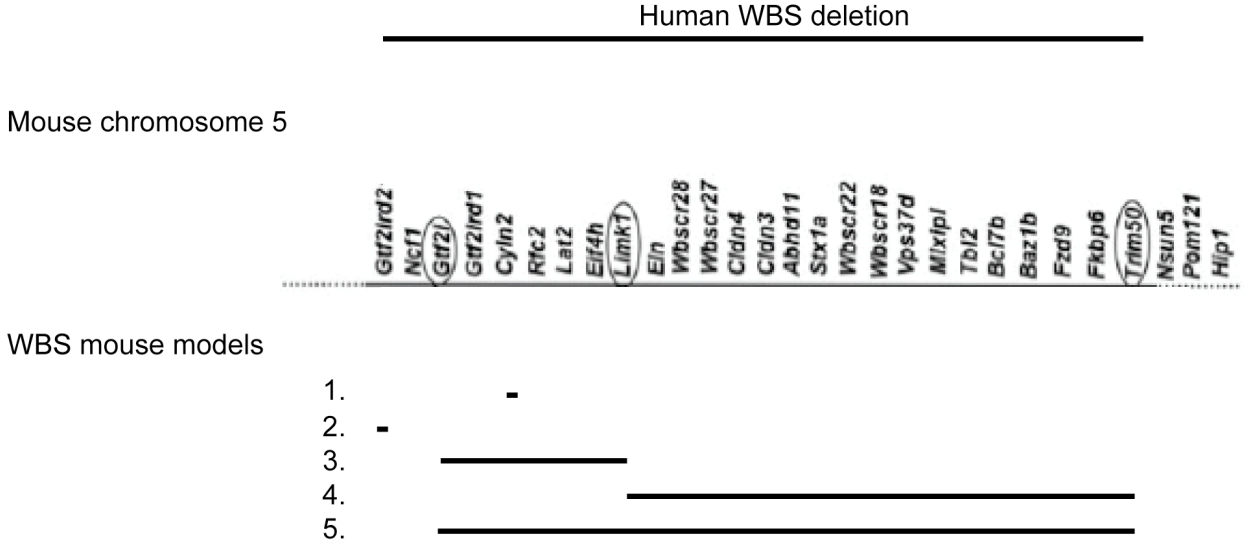

Figure 1.9. WBS mouse models that have been generated to date. Figure modified from Li *et al*., 2009.
Legend: 1. Mouse model heterozygous for *Cyln2* (Hoogenraad 2002); 2. Mouse model heterozygous for *Gtf2ird1* (Young 2008); 3. PD mouse model (mouse model heterozygous for *Gtf2i–Limk1*) (Li 2009); 4. DD mouse model (mouse model heterozygous for *Limk1–Fkbp6*) (Li 2009); 5. PD/DD mouse model mouse model heterozygous for *Gtf2i– Fkbp6*) (Li 2009).

Table 1.5. Brief summary of WBS mouse models that have been generated to date.

Clinical symptoms observed in humans with WBS	Mouse model heterozygous for *Cyln2* (Hoogenraad 2002)	Mouse model heterozygous for *Gtf2ird1* (Young 2008)	PD mouse model (Li 2009)	DD mouse model (Li 2009)	PD/DD mouse model (Li 2009)
Cardiovascular abnormalities	Not reported	Not reported	-	-*	-*
Craniofacial abnormalities	-	-	-	+	+
Intellectual disability	+	-	-	+	+
Behavioural problems	+	+	+	-	+
Motor impairment	+	Not reported	+	+	+
Weakness of connective tissues	Not reported	Not reported	-	+	+
Short stature	+	+	+	+	+
Reduced brain volume	-	-	+ (females)	+	+

* Although, monosomic DD and D/P mice did not show any cardiovascular abnormalities upon histopathological examination, significantly decreased anterior abdominal aortic wall motion was observed in both monosomic DD and D/P mice.

Mice carrying a heterozygous deletion of the *Cyln2* gene showed growth and motor deficiency, learning and behavioural impairment, brain anomalies, reduced synaptic plasticity, and hippocampal dysfunction (Hoogenraad 2002) (**Figure 1.9**), while mice with partial deletion of the *Gtf2ird1* gene displayed mild growth impairment and behavioural abnormalities (Young 2008) (**Figure 1.9**).

Two mouse models carrying a complimentary proximal (PD) and distal (DD) monosomic deletion syntenic to the genomic interval most commonly deleted in WBS patients have been generated using chromosome engineering (Li 2009) (**Figure 1.9**). The proximal deletion encompassed the region from *Gtf2i* to *Limk1* inclusively (monosomic PD mice), while the distal deletion spanned the region from *Limk1* to *Fkbp6* inclusively (monosomic DD mice). Also, the double heterozygous mice carrying both the proximal and distal deletion (monosomic D/P mice) (**Figure 1.9**), and thus carrying the deletion syntenic to the entire genomic interval most commonly deleted in WBS patients, were derived (Li 2009). Monosomic PD, DD and D/P mice showed

reduced body weight and impairment in motor skills and coordination. However, monosomic D/P mice displayed more severe growth retardation and more severe abnormalities in motor skills and coordination, suggesting that genes mapped to both PD and DD genomic intervals might be involved in the manifestation of these phenotypes. Monosomic PD and D/P, but not DD mice, showed increased social interest, indicating that genes in the PD region are likely to contribute to the development of increased sociability observed in WBS individuals. Monosomic DD and D/P, but not PD mice, had shorter skulls, showed reduced overall brain weight and learning impairment suggesting that genes in the DD region are likely to be responsible for the development of craniofacial abnormalities, reduced brain weight and intellectual disability observed in WBS patients. Interestingly, the existing genotype-phenotype correlation, suggesting that the deficiency or disruption of the *ELN* gene leads to supravalvular aortic stenosis in humans, has been challenged by monosomic DD and D/P mouse models, and thus by mice carrying deletions encompassing the *Eln* gene, as monosomic DD and D/P mice did not show any cardiovascular abnormalities upon histopathological examination. On the other hand, as significantly decreased anterior abdominal aortic wall motion was observed in both monosomic DD and D/P mice, the contribution of the *Eln* gene to the development of supravalvular aortic stenosis cannot be excluded. Altogether, these three mouse models recapitulated several phenotypes observed in WBS individuals, and helped to narrow down the genomic region, where dosage-sensitive genes responsible for different aspects of WBS can be further searched.

Mouse models have both advantages and disadvantages. On the one hand, the currently existing mouse models carrying defined chromosomal deletions have greatly improved our understanding of the molecular and cellular basis of some human deletion syndromes. They have also helped to identify causal genes responsible for the development of at least some of the clinical manifestations that are observed in patients. For example, a sequential development of mouse models for DiGeorge syndrome led to the identification of the *Tbx1* gene as responsible for cardiovascular abnormalities diagnosed in DGS individuals. Other mouse models helped to narrow down the genomic

intervals within which causative genes contributing to the development of clinical phenotypes identified in humans occur. For example, phenotypic analysis of the PD and DD mouse models of Williams syndrome identified a correlation between increased sociability observed in WBS individuals and the deletion of genes within the PD interval, and established a link between craniofacial abnormalities, reduced brain weight and intellectual disability observed in WBS patients with the deletion of genes mapped within the DD interval.

However, on the other hand, we need to be aware of the limitations that we might encounter when using mice as a model organism. In many instances mouse models recapitulated only a subset of clinical manifestation observed in patients with genomic disorders. For example, hypogonadism and obesity, two cardinal clinical manifestations observed in patients with Prader-Willi syndrome, have never been identified in any of the PWS mouse models, despite the fact that at least eight mouse models of Prader-Willi syndrome, each carrying a different chromosomal rearrangement, have been generated. The inability to recapitulate some of the clinical phenotypes identified in patients with deletion syndromes clearly suggests the existence of significant developmental differences between mice and humans, and thus places certain limitations on the use of mice as a model organism (at least in some cases). Also, we need to be aware that certain phenotypic features that are observed in humans with genomic disorders might be impossible to model or reliably identify in mice. For example, facial abnormalities, such as almond-shaped eyes and triangular mouth observed in PWS patients or full cheeks, prominent lips and wide mouth observed in DGS individuals cannot be reliably modelled in mice due to significant differences in facial appearance between mice and humans.

In some instances several mouse models of the same syndrome have been generated. For example, in PWS syndrome at least eight mouse models were generated. This is for two reasons. Firstly, by initially deleting a large region and then progressively generating models with smaller and smaller deletions, it is possible to narrow down the region within which the causative gene might be found. Secondly, although mouse models may carry the same deletion, they might have a different genetic background, and this could in

some circumstances lead to different manifestations of the clinical phenotypes observed in humans.

Despite the success of mouse models, there are still many questions that remain to be answered. For example, although the relevant gene has been identified in PWS syndrome, the mouse model does not recapitulate many of the clinical manifestations of the human phenotype. Perhaps it would be interesting to model this deletion in another organism, perhaps one closer to humans, which might better capture the observed human phenotype.

To sum up, there are still many human deletion syndromes, such as Sotos syndrome and Monosomy 21 syndrome, which remain to be modelled in mice. The generation of these will hopefully lead to genotype-phenotype correlations and to an increased insight into the development and pathophysiology of these disease phenotypes.